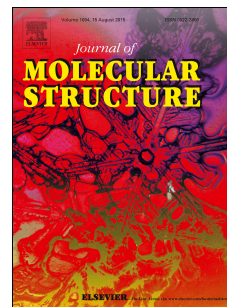


Accepted Manuscript

Design, synthesis and anti-inflammatory activity of pyrimidine scaffold benzamide derivatives as epidermal growth factor receptor tyrosine kinase inhibitors

K. Thirumurugan, Sivalingam Lakshmanan, Dharman Govindaraj, D. Sam Daniel Prabu, N. Ramalakshmi, S. Arul Antony



PII: S0022-2860(18)30704-X

DOI: [10.1016/j.molstruc.2018.06.003](https://doi.org/10.1016/j.molstruc.2018.06.003)

Reference: MOLSTR 25290

To appear in: *Journal of Molecular Structure*

Received Date: 16 March 2018

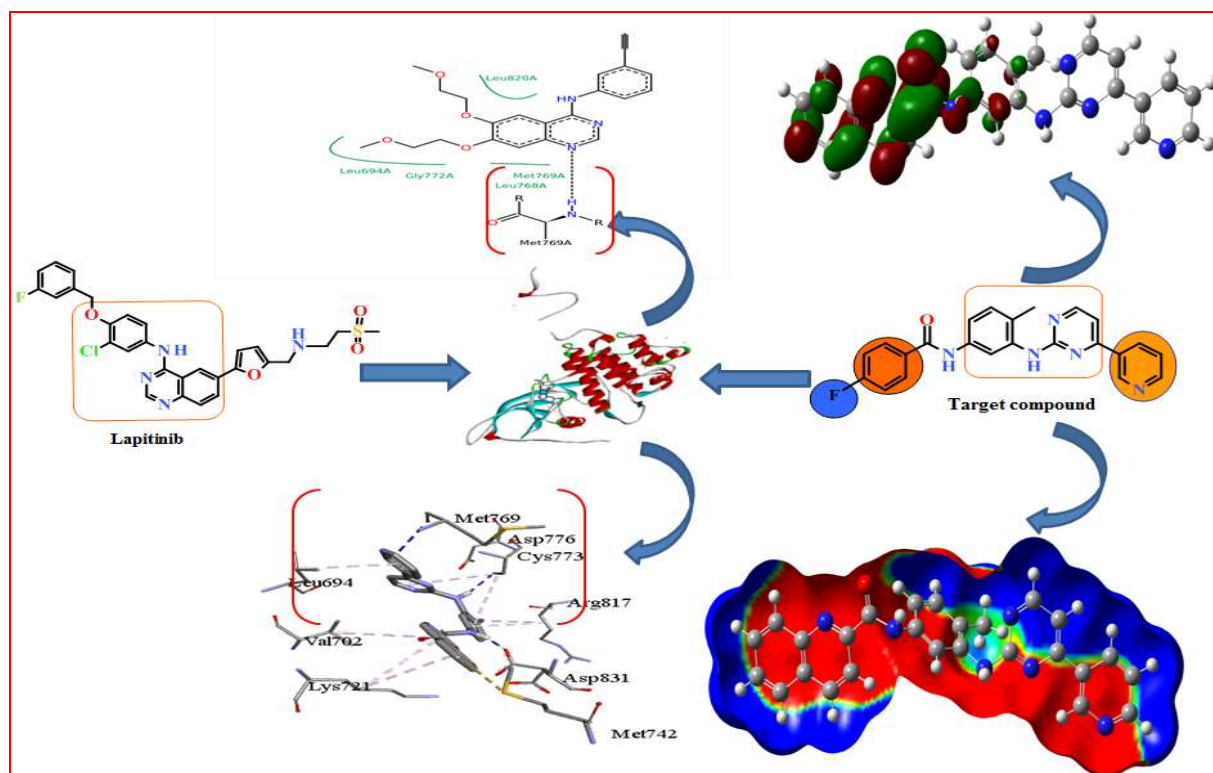
Revised Date: 12 May 2018

Accepted Date: 1 June 2018

Please cite this article as: K. Thirumurugan, S. Lakshmanan, D. Govindaraj, D.S. Daniel Prabu, N. Ramalakshmi, S. Arul Antony, Design, synthesis and anti-inflammatory activity of pyrimidine scaffold benzamide derivatives as epidermal growth factor receptor tyrosine kinase inhibitors, *Journal of Molecular Structure* (2018), doi: [10.1016/j.molstruc.2018.06.003](https://doi.org/10.1016/j.molstruc.2018.06.003).

This is a PDF file of an unedited manuscript that has been accepted for publication. As a service to our customers we are providing this early version of the manuscript. The manuscript will undergo copyediting, typesetting, and review of the resulting proof before it is published in its final form. Please note that during the production process errors may be discovered which could affect the content, and all legal disclaimers that apply to the journal pertain.

Graphical Abstract



ACCEPTED

Design, Synthesis and Anti-inflammatory Activity of Pyrimidine Scaffold Benzamide Derivatives as Epidermal Growth Factor Receptor Tyrosine Kinase Inhibitors[†]

K. Thirumurugan^a, Sivalingam Lakshmanan^a, Dharman Govindaraj^b, D. Sam Daniel Prabu^a, N. Ramalakshmi^{a,*}, S. Arul Antony^a

^a **Post-Graduate and Research Department of Chemistry, Presidency College, Chennai-05, Tamil Nadu, India.*

^b *Biomaterials in Medicinal Chemistry Lab, Department of Natural Products Chemistry, School of Chemistry, Madurai Kamaraj University, Madurai, 625021, India.*

*Email address: lachuchem666@gmail.com; Tel: +91 9843632843

Abstract

Novel series of pyrimidine scaffold benzamide derivatives (**9 a-k**) were synthesized and characterized by IR, HRMS, and NMR. Docking study of compounds **9 g**, **9 h** exhibited H-bonding interacts with Met769 into ATP binding site of EGFR-TK which showed similar binding mode to Lapitinib (PDB code: 1M17). Results indicated the ability to potent and selective inhibitors of the Epidermal Growth Factor Receptor tyrosine kinase (EGFR-TK). The molecular electrostatic potential (MEP), frontier molecular orbitals (FMOs) and HOMO-LUMO energy gap of the title compounds were investigated by using the B3LYP/6-31G method. The synthesized compounds were screened for *in vitro* anti-inflammatory activity.

Keywords: Microwave method; Pyrimidine scaffold benzamide; Molecular docking; DFT; MEPs; EGFR-inhibitors; Anti-inflammatory.

1. Introduction

Cancer is continuing to be a major health problem in developed as well as undeveloped countries [1]. The great cancer incidence worldwide increases the search for new, safer and efficient anticancer agents, aiming the prevention or the cure of this illness. Generally, curing of cancer is difficult because of the side effect of drugs on the normal cells and makes some other abnormalities in our body. Lung cancers are malignant tumours with poor prognoses and ranked as the top cause of cancer-related deaths [2, 3]. Inhibitors of the EGFR PTK are therefore expected to have great therapeutic potential in the treatment of malignant and nonmalignant epithelial diseases [4, 5]. One of the most prominent protein kinases is the endothelial growth factor receptor (EGFR) because that kinase is known to be involved in the various cancer-associated processes of uncontrolled cell growth [6, 7]. EGFR inhibitors are well-known active targets and to be efficient in the drug development for the treatment of cancer [8-10]. EGFR-TK inhibitors are the second most essential drug targets have been approved for the therapy of non-small cell lung cancer and this motivated inhibition of EGFR signaling may not only active in anti-proliferative effects and have also been increased sensitivity to cytotoxic therapies [11]. In recent days, various approaches have been developed to small molecule inhibitors of the intrinsic tyrosine kinase domain-like Lapatinib **(a)**, Erlotinib **(b)**, Gefitinib **(c)**, **Figure 1** which has been approved for the chemotherapeutic treatment of patients with advanced non-small lung cancer [12] and also Lapatinib **(a)** is a potent dual EGFR/ErbB2 inhibitor, recently approved by US Food and Drug Administration (FDA) for the breast cancer therapy [13]. The epidermal growth factor receptor (EGFR) is cellular trans-membrane tyrosine kinases that are over-expressed in a significant number of human tumors (e.g., Colon, breast, ovarian and NSC lung cancer) [14]. Therefore, EGFR

inhibitors represent a sensible approach for the development of novel anticancer therapies which would act by competing with ATP for binding at the catalytic domain of their target enzyme [15-17].

<< **Figure 1** >>

In recent years, various nitrogen heterocyclic rings are known to exhibit interesting biological activities. Pyrimidine is an important class of heterocyclic ring is found in vitamins like thiamine, riboflavin and folic acid. During the last two decades, several pyrimidine derivatives have been developed as chemotherapy of AIDS [18]. The previously reported literature presented that different structured fused pyrimidine ring systems are highly active in numerous chemotherapeutic activities such as anti-cancer [19, 20], antibacterial [21, 22], antifungal [23, 24], and anti-viral [25, 26] applications. The substituted pyrimidine ring systems were also reported to possess excellent antitumor activity [27-29]. Literature evaluations have pointed out the inherited antitumor potency of compounds containing pyrimidine and fused quinazoline moieties [30-32]. FDA has been approved for several quinazoline derivatives as anticancer drugs (e.g., Gefitinib, Erlotinib, Lapatinib and Vandetanib). Nowadays, the bio-medicinal activity of quinazoline derivatives and drug development of novel quinazoline derivatives for the anticancer therapy is a promising field [33-35].

The present work, we have carried out the chemical modifications on the general features of quinazoline-containing compounds. These modifications involve a replacement of the furan moiety in the quinazoline skeleton by pyrimidine scaffold benzamide moiety to develop more effective target molecules utilizing a fragment-based drug design approach and biologically evaluated their anti-inflammatory activity **Figure 2**.

<< **Figure 2** >>

2. Experimental

2.1. Materials and methods

All the solvents and chemicals were used analytical grade from SRL and Merck Ltd. Microwave reactions were performed with a Biotage®. Initiator with a continuous focused microwave power delivery system in a pressure glass vessel (10 mL) sealed with a septum under magnetic stirring. TLC was performed on commercial Merck silica gel 60 F 254. Column chromatography was carried out using silica gel 60-120 mesh. ¹HNMR spectra were recorded in CDCl₃ and DMSO-d₆ using TMS an internal standard with Bruker 300 MHz NMR spectrometer. High-resolution mass spectra (HRMS) were measured on a Finnigan spectrometer.

2.2. 3-(Dimethylamino)-1-(pyridin-3-yl)prop-2-en-1-one (3)

The mixture of N, N-dimethylformamide dimethylacetal (0.02 mol), acetylpyridine (0.01 mol), and toluene (3.5 mL) in a 10 mL glass vial well equipped. The reaction mixture was irradiated in the microwave synthesizer at 120 °C for 15 mins. After completion of the reaction (indicated by TLC), the mixture was cooled down to room temperature. Petroleum ether (2 mL) was added to the reaction mixture and kept stirring for 20 min. The resultant solid was collected by filtration and washed with hexane to get compound (3). Melting point 83-85 °C, ES-MS (M+1) found (m/z): 177.1.

2.3. 4-(Pyridin-3-yl)pyrimidin-2-amine (4)

The obtained compound **3** followed by 3-(dimethylamino)-1-(pyridin-3-yl) prop-2-en-1-one (0.1 mol), guanidine nitrate (0.1 mol), sodium hydroxide (0.1 mol), and n-butanol (12.5 mL) was irradiated in the microwave synthesizer at 90 °C for 20 mins. After completion of the reaction mixture poured into ice-cold water and the resulting solid was filtered and washed with water. The obtained solid of compound **4** (1.18 g) was dried under vacuum. Melting point 190-192 °C,

ES-MS (M+1) found (m/z): 173.1.

2.4. 2-Bromo-1-methyl-4-nitrobenzene (6)

The mixture of *P*-nitrotoluene (0.05 mol) and 0.1 g of iron powder in a 250 mL round bottom flask with compound 4 was heated at 80 °C with vigorous stirring and 3.0 mL (0.06 mol) of bromine was added over the period of 30-45 mins and heating continued for the course of 2 hrs. The reaction mixture was poured into 75 mL ice-cold 10% sodium hydroxide solution and the solid was heated with 25 mL of glacial acetic acid. The aqueous layer was decanted and the resulting solid was filtered and dried under vacuum to obtained 8.9 g (82 %) compound (6). Melting point 74-76 °C, ES-MS (M+1) found (m/z): 217.2.

2.5. N-(2-Methyl-5-nitrophenyl)-4-(pyridin-3-yl) pyrimidin-2-amine (7)

The mixture of 4-(Pyridin-3-yl) pyrimidin-2- amine (0.378 g, 2.2 mmol), copper iodide (0.5 mmol) and anhydrous K₂CO₃ (4 mmol), Dioxane (5 mL), 2-bromo-1-methyl-4-nitrobenzene (2 mmol), and DMEDA (0.5 mmol) was irradiated in the microwave synthesizer and heated at 120 °C for 30 mins. After completion of the reaction, ammonium hydroxide and brine solution was added and then extracted with ethyl acetate. The organic layer was dried over anhydrous sodium sulphate, the solvent was evaporated in buchi rotary evaporator and the resulting solid was dried under vacuum. The crude was purified by using silica gel column chromatography using ethyl acetate: chloroform (50:50) to yield 0.498 g (79.0 %) of the imatinib intermediate compound as yellowish powder. Melting point 194-196 °C. ES-MS (M+1) found (m/z): 308.1. ¹H-NMR (DMSO-d₆): 2.49(S, 3H); 7.32-7.37(m,1H); 7.40-7.48(m,1H); 7.49-7.51(m,1H); 7.85-7.88(m,1H); 8.02(m,1H); 8.48-8.51(m,1H); 8.57-8.59(m,1H); 9.20(S,1H); 9.29 (S,1H).

2.6. 6-Methyl-N-(4-(pyridin-3-yl)pyrimidin-2-yl)benzene-1,3-diamine (8)

The imatinib intermediate of N-(2-methyl-5-nitrophenyl) - 4-(pyridin-3-yl) pyrimidin-2-amine (1 mmol), was dissolved in THF followed by activated zinc (4 mmol) and ammonium chloride (10 mmol) were added. The reaction mixture was irradiated in the microwave synthesizer at 80 °C for 10 mins. After completion of the reaction filtered and washed with THF. The filtrate was evaporated and crude product was stirred with crushed ice. The resulting pale yellow precipitate was dried under vacuum (Yield, 0.208 g, 75.13 %); m.p. 142-144° C. ES-MS (M+1) found (m/z): 278.1. ¹H-NMR (DMSO-*d*₆): 2.16 (s, 3H); 4.44 (s, 2H); 6.39-6.41 (m, 1H); 6.91-6.93 (m, 1H); 7.15-7.18 (m, 1H); 7.22-7.23 (m, 1H); 7.92-7.94 (m, 1H); 8.12 8.13 (m, 1H); 8.46-8.48 (m, 1H); 8.68-8.69 (m, 1H); 9.26 (s, 1H).

2.7. General procedure for the synthesis of pyrimidine scaffold benzamide derivatives

(9 a-k)

The final target compounds were synthesized from 6-methyl- N-(4-(pyridin-3-yl) pyrimidin-2-yl) benzene-1,3-diamine **8** (2 mmol), DMF (10 mL), and DIPEA (4 mmol) followed by substituted aromatic acid (2 mmol) was added and stirred at room temperature for 1 hr. After completion of the reaction mixture was poured into ice-cold water. The obtained yellow precipitate washed with water and dried to get target titled product pyrimidine scaffold benzamide derivatives (**9 a-k**).

2.7.1. N-(4-methyl-3-((4-(pyridin-3-yl)pyrimidin-2-yl)amino)phenyl)picolinamide (**9 a**)

Yellow solid, Yield 90 %, FTIR (KBr, ν cm^{-1}): 2360 (-C-H), 1644 (-C=O), 1585 (-N-H), 1549 (C=N), 1132 (C-N). ¹H-NMR (300MHz, CDCl₃) δ 9.80 (s, 1H), 9.01(s, 1H), 8.50-8.45 (m, 2H), 8.37-8.30 (m, 2H), 8.29-8.27 (m, 2H), 8.07 (d, J = 7.8 Hz, 1H), 7.66 (t, J = 7.7 Hz, 1H), 7.24 - 7.16 (m, 2H), 7.00 (d, J = 8.2 Hz, 2H), 6.94 (d, J = 5.2 Hz, 1H), 2.10 (s, 3H). ES-MS (M+1) Calculated (m/z) 382.15, Found 383.1. Anal. Calcd. For

C₂₂H₁₈N₆O: C, 69.10; H, 4.74; N, 21.98%; Found: C, 69.06; H, 4.72; N, 21.99%.

2.7.2. 4-methyl-N-(4-methyl-3-((4-(pyridin-3-yl)pyrimidin-2-yl)amino)phenyl)benzamide (9 b)

Yellow solid, Yield 88 %, FTIR (KBr, ν cm⁻¹): 2361(-C-H), 1645 (-C=O), 1534 (-N-H), 1451(C=N), 1133 (C-N). ¹H NMR (300 MHz, CDCl₃) δ 8.98 (s, 1H), 8.44 (br, 1H), 8.34-8.25 (m, 3H), 7.71 (s, 1H), 7.53 (d, J = 7.8 Hz, 1H), 7.19 -7.12 (m, 1H), 7.07-7.02 (m, 3H), 6.96-6.81 (m, 4H), 2.17 (s, 3H), 2.10 (s, 3H). ES-MS (M+1) Calculated (m/z) 395.17, Found 396.10. Anal. Calcd. For C₂₄H₂₁N₅O: C, 72.89; H, 5.35; N, 17.71% Found: C, 72.86; H, 5.36; N, 17.73%.

2.7.3. 2-methyl-N-(4-methyl-3-((4-(pyridin-3-yl)pyrimidin-2-yl)amino)phenyl)benzamide (9 c)

Yellow solid, Yield 92 %, FTIR (KBr, ν cm⁻¹): 2361(-C-H), 1639 (-C=O), 1534 (-N-H), 1448 (C=N), 1133 (C-N). ¹H NMR (300MHz, CDCl₃) δ 8.91 (s, 1H), 8.39 (br, 1H), 8.33-8.23 (m, 3H), 7.66 (s, 1H), 7.24 (d, J = 7.4 Hz, 1H), 7.15-7.10 (m, 2H), 7.08-7.06 (m, 2H), 6.99-6.94 (m, 2H), 6.90-6.84 (m, 2H), 2.27 (s, 3H), 2.10 (s, 3H). ES-MS (M+1) Calculated (m/z) 395.17, Found 396.12. Anal. Calcd. For C₂₄H₂₁N₅O: C, 72.89; H, 5.35; N, 17.71 % Found: C, 72.86; H, 5.36; N, 17.72 %.

2.7.4. 4-chloro-N-(4-methyl-3-((4-(pyridin-3-yl)pyrimidin-2-yl)amino)phenyl)benzamide (9 d)

Yellow solid, Yield 82 %, FTIR (KBr, ν cm⁻¹): 2361(-C-H), 1644 (-C=O), 1535 (-N-H), 1449 (C=N), 1132 (C-N). ¹H NMR (300 MHz, CDCl₃) 8.99 (s, 1H), 8.44 (br,1H), 8.33-8.21 (m, 3H), 7.96 (s, 1H), 7.56 (d, J = 8.1Hz, 2H), 7.16 (d, J = 6.9 Hz, 2H), 7.04-6.92 (m, 2H), 6.90-6.84 (m,2H). 2.10 (s, 3H). ES-MS (M+1) Calculated (m/z) 415.12, Found

416.1. Anal. Calcd. For $C_{23}H_{18}ClN_5O$: C, 66.43; H, 4.36; N, 16.84 % Found: C, 66.41; H, 4.35; N, 16.86 %.

2.7.5. 4-methoxy-N-(4-methyl-3-((4-(pyridin-3-yl)pyrimidin-2-yl)amino)phenyl)benzamide (9 e)

Yellow solid, Yield 90%, FTIR (KBr, ν cm^{-1}): 2361(-C-H), 1643 (-C=O), 1534 (-N-H), 1449 (C=N), 1119 (C-N). 1H NMR (300 MHz, $CDCl_3$) δ 9.00 (s, 1H), 8.45 (br, 1H), 8.33-8.25 (m, 3H), 7.70 (s, 1H), 7.62 (d, $J = 9.0$ Hz, 2H), 7.20-7.15 (m, 1H), 7.08-7.02 (m, 2H), 6.96-6.91 (m, 2H), 6.82-6.70 (m, 2H), 3.62 (s, 3H), 2.10 (s, 3H). ES-MS (M+1) Calculated (m/z) 411.17, Found 412.1. Anal. Calcd. For $C_{24}H_{21}N_5O_2$: C, 70.06; H, 5.14; N, 17.02% Found: C, 70.09; H, 5.16; N, 17.01%.

2.7.6. 3-chloro-N-(4-methyl-3-((4-(pyridin-3-yl)pyrimidin-2-yl)amino)phenyl)benzamide (9 f)

Yellow solid, Yield 94 %, FTIR (KBr, ν cm^{-1}): 2361(-C-H), 1662 (-C=O), 1549 (-N-H), 1444(C=N), 1127 (C-N). 1H NMR (300 MHz, $CDCl_3$) δ 9.00 (s, 1H), 8.45 (br, 1H), 8.35-8.23 (m, 3H), 7.96 (s, 1H), 7.62 (s, 1H), 7.51 (d, $J = 7.6$ Hz, 1H), 7.26-7.15 (m, 3H), 7.11-7.04 (m, 2H), 6.97-6.86 (m, 2H), 2.10 (s, 3H). ES-MS (M+1) Calculated (m/z) 415.12, Found 416.1. Anal. Calcd. For $C_{23}H_{18}ClN_5O$: C, 66.43; H, 4.36; N, 16.84% Found: C, 66.41; H, 4.37; N, 16.82%.

2.7.7. 4-fluoro-N-(4-methyl-3-((4-(pyridin-3-yl)pyrimidin-2-yl)amino)phenyl)benzamide (9 g)

Yellow solid, Yield 87 %, FTIR (KBr, ν cm^{-1}): 2361(-C-H), 1654 (-C=O), 1538 (-N-H), 1446 (C=N), 1124 (C-N). 1H NMR (300 MHz, $CDCl_3$) δ 9.01 (s, 1H), 8.44 (br, 1H), 8.34-8.23 (m, 3H), 7.82 (s, 1H), 7.65 (dd, $J = 8.5, 5.3$ Hz, 2H), 7.18-7.14 (m, 1H), 7.02-

6.93 (m, 3H), 6.92- 6.83 (m, 3H), 2.10 (s, 3H). ES-MS (M+1) Calculated (m/z) 399.15, Found 400.1. Anal. Calcd. For C₂₃H₁₈FN₅O: C, 69.16; H, 4.54; N, 17.53% Found: C, 69.19; H, 4.52; N, 17.55 %.

2.7.8. N-(4-methyl-3-((4-(pyridin-3-yl)pyrimidin-2-yl)amino)phenyl)quinoline-2-carboxamide (9 h)

Yellow solid, Yield 84 %, (KBr, ν cm⁻¹): 2362 (-C-H), 1644 (-C=O), 1549 (-N-H), 1448 (C=N), 1176 (C-N). ¹H NMR (300 MHz, CDCl₃) δ 10.00 (s, 1H), 9.02 (s, 1H), 8.55 (s, 1H), 8.44 (br, 1H), 8.33-8.27 (m, 2H), 8.17 – 8.09 (m, 3H), 7.91 (d, 6.0 Hz, 1H), 7.64 (d, J = 8.2 Hz, 1H), 7.52 (t, J = 6.0Hz, 1H), 7.37 (t, J = 7.8 Hz, 1H), 7.27-7.15 (m, 2H), 7.00-6.96 (m, 1H), 6.92-6.86 (m, 1H), 2.10 (s, 3H). ES-MS (M+1) Calculated (m/z) 432.17, Found 433.1. Anal. Calcd. For C₂₆H₂₀N₆O: C, 72.21; H, 4.66; N, 19.43% Found: C, 72.25; H, 4.67; N, 19.45 %.

2.7.9. N-(4-methyl-3-((4-(pyridin-3-yl)pyrimidin-2-yl)amino)phenyl)pyrazine-2-carboxamide (9 i)

Yellow solid, Yield 90 %, FTIR (KBr, ν cm⁻¹): 2361(-C-H), 1644 (-C=O), 1587 (-N-H), 1450 (C=N), 1128 (C-N). ¹H NMR (300 MHz, CDCl₃) 9.38 (s, 1H), 9.11 (s, 1H), 8.66-8.55 (m, 2H), 8.45-8.17 (m, 3H), 7.45 (s, 1H), 7.29-7.22(m, 2H), 7.00-6.94 (m, 2H), 6.88-6.83 (m, 2H), 2.10 (s, 3H). ES-MS (M+1) Calculated (m/z) 383.15, Found 384.1. Anal. Calcd. For C₂₁H₁₇N₇O: C, 65.79; H, 4.47; N, 25.57% Found: C, 65.81; H, 4.49; N, 25.55 %.

2.7.10. 2-chloro-N-(4-methyl-3-((4-(pyridin-3-yl)pyrimidin-2-yl)amino)phenyl)benzamide (9 j)

Yellow solid, Yield 92 %, FTIR (KBr, ν cm⁻¹): 2361(-C-H), 1644 (-C=O), 1549 (-N-H),

1449 (C=N), 1157 (C-N). ¹H NMR (300 MHz, CDCl₃) 8.93 (s, 1H), 8.42 (br, 1H), 8.35 – 8.24 (m, 2H), 7.89 (s, 1H), 7.53 (d, J= 6.6 Hz, 1H), 7.15-7.07 (m, 3H), 7.01-6.97 (m, 2H), 6.93-6.91 (m, 2H), 6.87-6.83 (m, 2H), 2.10 (s, 3H). ES-MS (M+1) Calculated (m/z) 415.12, Found 416.1. Anal. Calcd. For C₂₃H₁₈ClN₅O: C, 66.43; H, 4.36; N, 16.84% Found: C, 66.45; H, 4.35; N, 16.82 %.

2.7.11. N-(4-methyl-3-((4-(pyridin-3-yl)pyrimidin-2-yl)amino)phenyl)benzamide (**9 k**)

Yellow solid, Yield 90 %, FTIR (KBr, v cm⁻¹): 2361(-C-H), 1671 (-C=O), 1531(-N-H), 1447 (C=N), 1129 (C-N). ¹H NMR (300 MHz, CDCl₃) δ 9.00 (s, 1H), 8.45-8.35 (m, 3H), 8.27 (br, 2H), 7.88 (s, 1H), 7.66-7.61 (m, 2H), 7.38-7.16 (m, 5H), 6.95-6.91 (m, 2H), 2.10 (s, 3H). ES-MS (M+1) Calculated (m/z) 381.16, Found 382.1. Anal. Calcd. For C₂₃H₁₉N₅O: C, 72.42; H, 5.02; N, 18.36% Found: C, 72.43; H, 5.01; N, 18.35 %.

3. Result and Discussion

3.1. Chemistry

The synthetic route for the newly synthesized compounds (**9 a-k**) was exhibited and outlined in **Scheme 1**. The microwave-assisted strategy with Ullmann reactions was performed by using a scientific microwave synthesizer. All the compounds were prepared by Loiseleur's method [36], microwave irradiation of N,N-dimethylformamide dimethylacetal, acetyl pyridine in toluene afforded 3-(Dimethylamino)-1-(pyridin-3-yl)prop-2-en-1-one (**3**). The cyclisation of compound (**3**) with guanidine nitrate in the presence of sodium hydroxide provided 4-(Pyridin-3-yl)pyrimidin-2-amine (**4**) was obtained in good yields. 2-Bromo-1-methyl-4-nitrobenzene (**6**) was prepared by reaction with iron powder and bromine. This reaction was performed in a conventional way, due to the evaporation of HBr as the by-product.

The Ullmann type reaction was performed and 4-(Pyridin-3-yl) pyrimidin-2-amine (**4**) reacts

under microwave irradiation with 2-Bromo-1-methyl-4-nitrobenzene (**6**) in the presence of copper iodide gave excellent yields. In this reaction, copper iodide used as a catalyst, potassium iodide as accelerant and N, N'-dimethylethylenediamine as a ligand and the reaction has proceeded in dioxane at 120 °C for 30 mins gave N-(2-Methyl-5-nitrophenyl)-4-(pyridin-3-yl)pyrimidin-2-amine (**7**) with 79 % yield. The ¹H-NMR spectrum of compound (**7**) showed a singlet (3H) at 2.49 and aromatic protons assigned in the region of 7.32 - 9.29 ppm. Reduction reaction of nitro compounds was performed by Fe and Zn in the presence of acids. The Zn/NH₄Cl method efficiently produced a good quantity of the expected amine (**8**). This was confirmed by the appearance of -NH₂ group at 4.44 ppm. The final product (**9 a-k**) was easily obtained by peptide coupling reaction of amine using TBTU and diisopropylethylamine corresponding acid gave excellent yield. All target synthesized pyrimidine scaffold benzamide derivatives (**9 a-k**) listed in **Figure 3**.

<< **Scheme 1** >>

<< **Figure 3** >>

4. Molecular docking

Molecular docking methodology was used to identify the structural features required for EGFR receptor bearing quinazoline inhibitor (PDB ID: 1M17(*Lapatinib*)) were studied **Figure 2**. It was found that a hydrogen bond acceptor of quinazoline ring interacts with Met769 [37]. The crystal structure of epidermal growth factor receptor with erlotinib (TarcevaTM) (PDB code: 1M17) [38-41].

The docking study of synthesized compounds with receptor RTK exhibited well-established bonds with one or more amino acids in the receptor active pocket. The compounds **9 a**, **9 d**, and **9 h** show very high binding energy with the RTK (1m17) receptor in **Figure 4**. The

compound **9 a** exhibits binding energy value -8.20 kcal/mol showed two H-bonding with Glu734, Lys721 as well as the strong affinity of Asp831, Val702, which results from two hydrophobic interaction its reduced the hydrogen bond interaction of compound **9 a** with RTK receptor. The quinoline containing compound **9 h** also exhibits strong binding energy -9.64kcal/mol which result four H-bonding with Asp831, Cys773, Met769, Met742 and as well as Asp776, Asp831, Arg817, Leu649, Cys773, Val702 and Lys721 amino acids, which results hydrophobic and electrostatic interactions to responsible for more activity of RTK receptor and its indicated that the presence of the bi-cyclic hetero nucleus has higher affinity for RTK protein.

The electron donating group of compound **9 e** shows binding energy -9.41 kcal/mol exhibited H-bonding with Asp831, Asn818, Arg817, Cys773 showed four hydrogen bond. The molecule was deeply embedded in the hydrophobic pocket formed by Phe771, Gly772, Glu780 exhibits hydrophobic bond with a chlorine atom, which result shows highest anti-inflammatory activity. The electron withdrawing compound **9 f** shows very low binding energy value -5.31 kcal/mol interact with amino acids Asp776, Cys773 shows two H-bonding compare to electron donating compound **9 g**. The compound **9 g** exhibits highest binding energy value -8.18k cal/mol interact with four hydrogen-bonded amino acid residue Met769, Cys773, Asp831, Thr766 and inside of strong hydrophobic interaction with Arg817, Asp831, Cys773, Leu694, Val702 and Lys721 amino acid residue, due to the presence of electron donating group in phenyl ring at para position. The order of binding affinity of docked benzamide derivatives against the RTK receptor is **9 h** > **9 d** > **9 a** > **9 g** > **9 e** > **9 c** > **9 i** > **9 k** > **9 j** > **9 b** and **9 f** with the range of binding energy being -9.64 to -5.96 kcal/mol. Generally, the functional groups (amine and ketone) are forming the hydrogen bond with amino acid residues **Figure 5**. The free energy of binding (FEB) of all compounds was calculated **Table 1**.

<< **Figure 4** >><< **Table 1** >><< **Figure 5** >>

5. Density Functional Theory

Theoretical calculations were performed by the density functional theory (DFT) method at the B3LYP/ 6-31G level of theory in the Gaussian 03 package of programs [42].

Density functional theory (DFT) which is one of these methods has been widely used in literature because of its efficiency and accuracy with respect to the evaluation of a number of molecular properties. The highest occupied molecular orbital (HOMO) and the lowest unoccupied molecular orbital (LUMO) reveal the biological potency of a molecule. Extending the concept to binding in drug-receptor systems. The extents of these stabilizing interactions are inversely related to the energy gap between the interacting orbitals. Higher HOMO energy and lower LUMO energy in the drug molecule result in larger stabilizing interactions and hence binding with the receptor. The orbital energies of both HOMO and LUMO and their gap were calculated for all the molecules and are reported in **Table 2**. It is remarkable that compounds **9 c**, **9 d**, **9 g** and **9 h** having the lowest energy gap (ΔE) of 1.3938, 0.8131, 0.9532, and 0.3913eV, respectively, exhibit the highest anti-inflammatory activity [43-47].

We also obtained a plot of the HOMO and LUMO of the molecules of each group to analyze the main atomic contributions for these orbitals. The importance of observing these plots was to determine which atoms were located at the possible sites of electronic transfer between the molecule under study and its biological target. The plots of the HOMO and LUMO of some molecules obtained from DFT calculations are displayed in **Figure 6**. The results illustrated that

HOMO molecular orbital of **9 a**, **9 d**, **9 g**, and **9 h** is mainly located in pyrimidine ring, indicating the existence of possible reactive sites; consequently, electrophilic attacks might take place on these sites. On the other hand, the LUMO is primarily concentrated on benzamide rings in which the negatively charged polar residues of the receptor are favorable, but HOMO of compound **9 g** presents similar characteristic, while the LUMO changes significantly. In this case, the LUMO is primarily located in Pyridine ring comparing with other compounds. This also implies that the orbital interaction between the target compound and the aromatic ring or some other side of residue chains of receptors is dominated by π - π or hydrophobic interaction. Moreover, anti-inflammatory activity is dependent on the low-lying E_{LUMO} because compound **9c** has the lowest E_{LUMO} value [48]. The compound **9j** size of the E_{HOMO} lobes located on the pyridine ring was significantly little smaller than that of compounds **9c** which result compound **9c** are likely to exhibit strong charge transfer, and good photosensitizers and therefore more active than **9j**.

<< **Figure 6** >>

<< **Table 2** >>

6. Molecular electrostatic potential surface (MEPs)

Molecular electrostatic potential (MEP) is related to the electronic density which is a very useful descriptor in understanding sites for nucleophilic reactions or electrophilic attack. In other words, they have been contemplated as an indicator of the reactivity regions of a target molecule; hence they have been employed in order to study electron-donator and electron-acceptor interactions between a drug and the amino acid residues of the target receptor [49].

As a result, this property was calculated for the target molecules at the B3LYP/6-31G level of theory, and indicated by a colour range from -2.420×10^{-3} (deepest blue) to $+2.420 \times 10^{-3}$ (deepest red) in the corresponding maps displayed. MEP is created by mapping of the

electrostatic potential on the total electron density of the molecules. For most active compounds **9 d**, **9 g** and **9 h** which shows in red the nucleophilic sites (negative potential), located at the oxygen atoms which result in H-bond interaction with the amino acid of target receptor. The large electrophilic sites (positive potential) appeared on the hydrogen attached to aromatic ring nitrogen consequence the blue cloud which is symbolized for electron deficient region. Due to the accumulation of positive potential, these moieties exhibited hydrophobic interactions with the aromatic residues of the active site in **Figure 7**. The other parts of molecule seem to potentially be less active in chemical point of view.

<< **Figure 7** >>

7. Anti-inflammatory activity

Heterocycles containing pyrimidine scaffold benzamide derivatives moiety are of great interest because they exhibit useful biological activities and clinical applications.

All the synthesized compounds were screened for their *in vitro* anti-inflammatory activity summarized in (**Table 1** and **Figure 8**). The tested compounds, **9 a**, **9 d**, **9 g**, **9 h**, and **9 i** were found significant activity when compared to the standard drug Diclofenac at their lower concentrations (10 μ M, 50 μ M, 100 μ M). The substitution of electron donating group Compounds **9 b**, **9 c** and **9 e** decreases the activity compared with the standard. The compound **9 h** much more active against anti-inflammatory in relation to Diclofenac sodium 89 % activity at the minimum concentration of 10 μ M. This may be the presence of bi-cyclic hetero nucleus of quinoline moiety [50]. Whereas compound **9 a** shows lower activity due to the presence of mono-heterocyclic of pyridine moiety. From the present study, it was noted that compound **9 d**, **9 g**, and **9 h** exhibited good anti-inflammatory.

<< **Figure 8** >>

8. Conclusion

In conclusion, novel pyrimidine scaffold benzamide derivatives have been synthesized and characterized. Theoretical investigation some electronic parameters including energies of HOMO-LUMO energy gaps and MEPs has exposed very clear trends between the molecular descriptor and inhibitory activity. SAR for analysis of nature of the substituent present on benzamide ring of lipophilic H-bond acceptor type functionalities like F, Cl at para position and the aromatic ring of lipophilic hydrophobic region (i.e. electron withdrawing group, pyridine, quinoline) of compounds **9 d**, **9 g**, and **9 h** significant structural motives leading to the moderately potent anti-inflammatory compounds. Moreover, molecular docking studies confirmed that compounds **9 d**, **9 g**, and **9 h** shared the similar binding pattern with Lapatinib in the binding pocket of EGFR. The obtained results suggested that compounds **9 d**, **9 g**, and **9 h** may be a promising lead for further modifications towards epidermal growth factor receptor (EGFR).

Acknowledgment

Authors have no financial interest.

Reference

1. L. Rahib, B. D. Smith, R. Aizenberg, A. B. Rosenzweig, J.M. Fleshman, L. M. Matrisian, Projecting Cancer Incidence and Deaths to 2030: The Unexpected Burden of Thyroid, Liver, and Pancreas Cancers in the United States, *Cancer Res.* 74 (2014) 2913-2921.
2. L. A. Torre, F. Bray, R. L. Siegel, J. Ferlay, J. L. Tieulent, A. Jemal, Global Cancer Statistics, 2012, *CA Cancer J. Clin.* 65 (2015) 87-108.

3. W. Chen, R. Zheng, P. D. Baade, S. Zhang, H. Zeng, F. Bray, A. Jemal, X. Q. Yu, J. He, Cancer statistics in China, 2015, *CA Cancer J. Clin.* 66 (2016) 115-132.
4. M. Starok, P. Preira, M. Vayssade, K. Haupt, L. Salome, C. Rossi, EGFR Inhibition by Curcumin in Cancer Cells: A Dual Mode of Action, *Biomac. mole.* 16 (2015) 1634-1642.
5. Rochelle Frankson, Zhi-Hong Yu, Yunpeng Bai, Qinglin Li, Ruo-Yu Zhang and Zhong-Yin Zhang , Therapeutic Targeting of Oncogenic Tyrosine Phosphatases, *Cancer Res.* 77 (2017) 5701-5705.
6. G. Banupriya, R. Sribalan, V. Padmini, Synthesis and characterization of curcumin-sulfonamide hybrids: Biological evaluation and molecular docking studies, *J. Mol. Struct.* 1155 (2018) 90-100.
7. R. M. Asath, R. Premkumar, T. Mathavan, A. M. F, Benial, Spectroscopic and molecular docking studies on N,N-Di-tert-butoxycarbonyl (Boc)-2-amino pyridine: A potential bioactive agent for lung cancer treatment, *J. Mol. Struct.* 1143 (2017) 415-423.
8. G. Wolber, T. Langer, 3D pharmacophores derived from protein-bound ligands and their use as virtual screening filters, *J. Chem. Inf. Comp. Sci.* 45 (2005) 160-169.
9. Y. Cheng, W. Cui, Q. Chen, C.H. Tung, M. Ji, F. Zhang, The molecular mechanism studies of chirality effect of PHA-739358 on Aurora kinase A by molecular dynamics simulation and free energy calculations, *J. Comput. Aided. Mol. Des.* 25 (2011) 171-180.
10. J.B. Johnston, S. Navaratnam, M.W. Pitz, J.M. Maniate, E. Wiechec, H. Baust, J. Gingerich, G.P. Skliris, L.C. Murphy, M. Los, Targeting the EGFR pathway therapy for cancer, *Curr. Med. Chem.* 13 (2006) 3483-3492.
11. F. Ciardiello, R. Caputo, R. Bianco, D. Vincenzo, G. Somatico, S. DePlacido, R.A. Bianco, G. Tortora, Antitumor Effect and Potentiation of Cytotoxic Drugs Activity in Human Cancer

- Cells by ZD-1839 (Iressa), an Epidermal Growth Factor Receptor-selective Tyrosine Kinase Inhibitor, *Clin. Cancer. Res.* 6 (2000) 2053-2063.
12. K. Abouzid, S. Shouman, Design, synthesis and in vitro antitumor activity of 4-aminoquinoline and 4-aminoquinazoline derivatives targeting EGFR tyrosine kinase, *Bioorg. Med. Chem.* 16 (2008) 7543-7551.
13. D.W. Rusnak, K. Lackey, K. Affleck, E.R. Wood, K.J. Alligood, N. Rhodes, B.R. Keith, D.M. Murray, W.B. Knight, R.J. Mullin, T.M. Gilmer, The Effects of the Novel, Reversible Epidermal Growth Factor Receptor/ErbB-2 Tyrosine Kinase Inhibitor, GW2016, on the Growth of Human Normal and Tumor-derived Cell Lines in Vitro and in Vivo, *Mol. Cancer. Ther.* 1 (2001) 85-94.
14. J.H. Cheng, C.F. Hung, S.C. Yang, J.P. Wang, S.J. Won, C.N. Lin, Synthesis and cytotoxic, antiinflammatory, and anti-oxidant activities of 2',5'-dialkoxychalcones as cancer chemopreventive agents, *Bioorganic & medicinal chemistry, Bioorg. Med. Chem.* 16 (2008) 7270-7276.
15. S. H. Myers, C. Temps, D. R. Houston, V. G. Brunton, A.U. Broceta, Development of Potent Inhibitors of Receptor Tyrosine Kinases by Ligand-Based Drug Design and Target-Biased Phenotypic Screening, *J. Med. Chem.* 61(2018) 2104-2110.
16. Y. Zhang, Y. Chen, D. Zhang, L. Wang, T. Lu, Y. Jiao, Discovery of Novel Potent VEGFR-2 Inhibitors Exerting Significant Antiproliferative Activity against Cancer Cell Lines, *J. Med. Chem.* 61 (2018) 140-157.
17. C. Hengmiao, S.K. Nair, B.W. Murray, Recent progress on third generation covalent EGFR inhibitors, *Bioorg. Med. Chem. Lett.* 26 (2016) 1861-1868.
18. K. S. Jain¹, T. S. Chitre¹, P. B. Miniyar¹, M. K. Kathiravan¹, V. S. Bendre¹, V. S. Veer, S.

- R. Shahane and C. J. Shishoo, Biological and medicinal significance of pyrimidines, *Curr. Sci.* 90 (2006) 793-803.
19. Rangel, C. D. Uribe, A. R. Serrano, X. Zarated, Y.Serge, W. Vallejo, M. Nogueras, J.Trilleras, J. Quirog, J. Tatchen, J. Cobo, Three-component one-pot synthesis of novel pyrido[2,3-d]pyrimidine indole substituted derivatives and DFT analysis, *J. Mol. Struct.* 1137 (2017) 431-439.
20. M. Wang, J.Yang, M.Yuan, L. Xue, H. Lia, C. Tiana, X. Wang, J. Liua, Z. Zhang, Synthesis and antiproliferative activity of a series of novel 6-substituted pyrido[3,2-d]pyrimidines as potential nonclassical lipophilic antifolates targeting dihydrofolate reductase, *Eur. J. Med. Chem.* 128 (2017) 88-97.
21. L. Suresh, P. S. Vijay Kumar, G.V.P. Chandramouli, An efficient one-pot synthesis, characterization and antibacterial activity of novel chromeno-pyrimidine derivatives, *J. Mol. Struct.* 1134 (2017) 51-58.
22. L. Suresha, P.S. Vijay Kumara, Y. Poornachandrab, C.Ganesh Kumar, G.V.P.Chandramouli, Design, synthesis and evaluation of novel pyrazolo pyrimido[4,5-d]pyrimidine derivatives as potent antibacterial and biofilm inhibitors, *Bioorg. Med. Chem. Lett.* 27 (2017) 1451-1457.
23. A. P.Keche, G.D.Hatnapure, R.H.Tale, A. H.Rodge, S. S.Birajdar, V. M.Kamble, A novel pyrimidine derivatives with aryl urea, thiourea and sulfonamide moieties: Synthesis, anti-inflammatory and antimicrobial evaluation, *J. Mol. Struct.* 22 (2012) 3445-3448.
24. C.Mallikarjunaswamy, L.Mallesha, D.G.Bhadregowda, OthbertPinto, Studies on synthesis of pyrimidine derivatives and their antimicrobial activity, *Ara. J. Chem.* 10 (2017) 484-490.

25. M. Krecmerova, M. Dracinsky, R. Snoeck, J. Balzarini, K.Pomeisl, G. Andrei, New prodrugs of two pyrimidine acyclic nucleoside phosphonates: Synthesis and antiviral activity, *Bioorg. Med. Chem.* 25 (2017) 4637-4648.
26. T. Li, J. Zhang, J. Pan, Z.Wu, D. Hu, B. Song, Design, synthesis, and antiviral activities of 1,5-benzothiazepine derivatives containing pyridine moiety, *Eur. J. Med. Chem.* 125 (2017) 657-662.
27. Z.H. Li, X.Q Liu, P.F.Geng, J.L. Ma, T.Q. Zhao, H.M. Wei, B. Yu, H.M. Liu, Design, synthesis, and biological evaluation of new thiazolo[5,4-d]pyrimidine derivatives as potent antiproliferative agents, *Med. Chem. Commun.* 8 (2017)1655-1658.
28. M. Said, K. Abouzid, A. Mouneer, A. Ahmedy, A.M. Osman, Synthesis and biological evaluation of new thiazolopyrimidines, *Arch. Pharm. Res.* 27 (2004) 471-477.
29. F. Tim, K. Thomas, N. Abdulkarim, T. Frank, S. Christoph, S. Wolfgang, R. Christoph, H. Andreas, Discovery of novel substituted benzo-anellated 4-benzylamino pyrrolopyrimidines as dual EGFR and VEGFR2 inhibitors, *Bioorg. Med. Chem. Lett.* 27 (2017) 2708-2712.
30. A.D. Settimo, F.D. Sattemo, A.M. Marini, G. Primofiore, S. Salerno, G. Viola, L.D. Via, S.M. Magno, Synthesis, DNA binding and in vitro antiproliferative activity of purinoquinazoline, pyridopyrimido purine and pyridopyrimidobenzimidazole derivatives as potential antitumor agents, *Eur. J. Med. Chem.* 33 (1998) 685-696.
31. V. Bavetsias, A.L. Jackman, J.H. Marriott, R. Kimbell, W. Gibson, F.T. Boyle, G.M. Bisset, Folate-based inhibitors of thymidylate synthase: synthesis and antitumor activity of g-linked sterically hindered dipeptide analogues of 2- desamino-2-methyl-N10-propargyl-5,8-dideazafolic acid (ICI 198583), *J. Med. Chem.* 40 (1997) 1495-1510.

32. M.J. Hour, L.J. Huang, S.C. Kuo, Y. Xia, K. Bastow, Y. Nakanishi, E. Hamel, K.H. Lee, 6-Alkylamino- and 2,3-dihydro-3'-methoxy-2-phenyl-4-quinazolines and related compounds: their synthesis, cytotoxicity and inhibition of tubulin polymerization, *J. Med. Chem.* 43 (2000) 4479-4487.
33. S. Lakshmanan, D. Govindaraj, N. Ramalakshmi, S. Arul Antony, Synthesis, Molecular docking, DFT calculations and Cytotoxicity activity of benzo[g]quinazoline derivatives in Choline Chloride-urea, *J. Mol. Struct.* 1150 (2017) 88-95.
34. S. Lakshmanan, N. Ramalakshmi, One-pot, four-component synthesis of benzylpyrazolyl naphthoquinone derivatives and molecular docking studies, *Synth. Commun.* 46 (2016) 2045-2052.
35. Z. Yaling, G. Hongliang, L. Renjie, L. Juan, C. Li, L. Xiabing, Z. Lijun, W. Wei, L. Baolin, Quinazoline-1-deoxynojirimycin hybrids as high active dual inhibitors of EGFR and α -glucosidase, *Bioorg. Med. Chem. Lett.* 27 (2017) 4309-4313.
36. S. Hanessian, G. Huang, C. Chenel, R. Machaalani, O. Loiseleur, Total Synthesis of N-Malayamycin A and Related Bicyclic Purine and Pyrimidine Nucleosides, *J. Org. Chem.* 70 (2005) 6721-6734.
37. J. Stamos, M.X. Sliwkowski, C. Eigenbrot, Structure of the epidermal growth factor receptor kinase domain alone and in complex with a 4-anilinoquinazoline inhibitor, *J. Biol. Chem.* 277 (2002) 46265-46272.
38. J. Fricker, Tyrosine kinase inhibitors: the next generation, *The Lancet Oncol.* 7 (2006) 621.
39. S. Garofalo, R. Rosa, R. Bianco, G. Tortora, EGFR-targeting agents in oncology, *Expert. Opin. Ther. Pat.* 18 (2008) 889-901.
40. S. Madhusudan, T. S.Ganesan, Tyrosine kinase inhibitors in cancer therapy, *Clin. Biochem.*

- 37 (2004) 618-635.
41. I.A. Al-Suwaidan, A.M. Alanazi, A.A.A. Aziz, A.M.A. Mohamed, A.S. El-Azab, Design, synthesis and biological evaluation of 2-mercapto-3-phenethylquinazoline bearing anilide fragments as potential antitumor agents: Molecular docking study, *Bioorg. Med. Chem. Lett.* 23 (2013) 3935-3941.
42. M.J. Frisch, G.W. Trucks, H.B. Schlegel, G.E. Scuseria, M.A. Robb, J.R. Cheeseman, Jr. J.A. Montgomery, T. Vreven, K.N. Kudin, J.C. Burant, Gaussian 03, Revision C. 01; Gaussian, Inc.: Wallingford, CT, USA, 2004.
43. S.H.R. Sebastian, M.A. Al-Alshaikh, A.A. El-Emam, C.Y. Panicker, J. Zitko, M. Dolezal, C.V. Alsenoy, Spectroscopic, quantum chemical studies, Fukui functions, in vitro antiviral activity and molecular docking of 5-chloro-N-(3-nitrophenyl)pyrazine-2-carboxamide, *J. Mol. Struct.* 1119 (2016) 188-199.
44. A. Ali, M. Asif, P. Alam, M.J. Alam, M.A. Sherwani, R.H. Khan, S. Ahmad, Shamsuzzaman, DFT/B3LYP calculations, in vitro cytotoxicity and antioxidant activities of steroidal pyrimidines and their interaction with HSA using molecular docking and multispectroscopic techniques, *Bioorg. Chem.* 73 (2017) 83-99.
45. M. Bavadi, K. Niknam, O. Shahraki, Novel pyrrole derivatives bearing sulfonamide groups: Synthesis in vitro cytotoxicity evaluation, molecular docking and DFT study, *J. Mol. Struct.* 1146 (2017) 242-253.
46. T. Kavitha, G. Velraj, Density functional theory analysis and molecular docking evaluation of 1-(2, 5-dichloro-4-sulfophenyl)-3-methyl-5-pyrazolone as COX2 inhibitor against inflammatory diseases, *J. Mol. Struct.* 1141 (2017) 335-345.
47. R.K. Singh, A.K. Singh, S. Siddiqui, M. Arshad, A. Jafri, Synthesis, molecular structure,

- spectral analysis and cytotoxic activity of two new aroylhydrazones, *J. Mol. Struct.* 1135 (2017) 82-97.
48. S. Bondock, H. Gieman, A. E. Shafei, Selective synthesis, structural studies and antitumor evaluation of some novel unsymmetrical 1-hetaryl-4-(2-chloroquinolin-3-yl)azines, *J. Sau. Chem. Soci.* 20 (2016) 695-702.
49. C. S. Correa, C. B. Salcedo, M. F. Marquez, C. I. S. Diaz, Computational study of substituent effects on the acidity, toxicity and chemical reactivity of bacteriostatic sulfonamides, *J. Mol. Grap. Mode.* 81 (2018) 116-124.
50. M.K. Nagy, A.A. Mohamed, A.A.E. Ahmed, M.A. El-Reheem, Anti-inflammatory and analgesic activities of some novel carboxamides derived from 2-phenyl quinoline candidates, *Biomed. Res.* 28 (2017) 869-874.

TABLE

Table.1. Docking results of novel biological active pyrimidine scaffold benzamide derivatives against tyrosine kinases inhibitor [1m17.pdb] protein.

Table.2. Energies of both HOMO and LUMO and their gaps (in eV) calculated for all synthesized compounds (9 a - k).

Table.1.

Compounds	Binding energy (kcal/mol)	No. of Hydrogen Bonding	<i>anti-inflammatory</i> (%) inhibition at 100 μ M
9a	-8.20	2	54.27
9b	-6.28	1	46.26
9c	-7.36	2	58.56
9d	-9.41	2	74.62
9e	-7.63	4	38.16
9f	-5.96	2	40.18
9g	-8.18	4	76.13
9h	-9.64	4	86.75
9i	-6.72	1	36.22
9j	-6.35	1	59.26
9k	-6.58	2	34.46
Diclofenac sodium	-	-	82.57

Table.2.

Compounds	E_{total} (kcal)	E_{HF}	μ (Debye)	E_{HOMO}	E_{LUMO}	ΔE
9a	-1252.2638		1.9632	-5.3747	-2.2362	3.1385
9b	-1275.5163		2.2611	-5.4395	-1.8773	3.5622
9c	-1274.8248		10.2240	-3.6240	-2.2302	1.3938
9d	-1695.3577		8.2076	-3.1938	-2.3807	0.8131
9e	-1350.7017		3.6058	-5.4512	-1.9037	3.5475
9f	-1695.7481		4.8668	-5.6518	-2.1997	3.4521
9g	-1334.8580		4.8082	-3.1249	-2.1717	0.9532
9h	-1267.9391		8.5707	-3.4621	-3.0708	0.3913
9i	-1405.9406		3.0235	-5.7211	-2.1331	3.594
9j	-1695.5669		7.6481	-3.7769	-2.5486	1.2283
9k	-1682.7321		4.6209	-5.7089	-2.2204	3.4885

FIGURE CAPTIONS

Fig.1. 4-Anilinoquinazolines EGFR-TK inhibitors, Lapitinib (**a**), Erlotinib (**b**), Gefitinib (**c**)

Fig.2. Design of target pyrimidine scaffolds benzamide compounds

Fig.3. Structure of synthesized pyrimidine scaffold benzamide derivatives (9 a-k)

Fig.4. Binding energy of synthesized compounds against tyrosine kinases inhibitor [1m17.pdb] protein

Fig.5. Molecular docking and amino acids interaction of the most active compounds 9 a, 9 d, 9 g and 9 h with RTK receptor. The amino acids involved in hydrogen (blue dashed line), hydrophobic (white) and electrostatic (red dashed line) interactions are highlighted.

Fig.6. Schematic representation of HOMO and LUMO coefficient distribution of 9 a, 9 d, 9 g and 9 h

Fig.7. Structure active relationships of Molecular electrostatic potential surface and amino acid interaction against target EGFR receptor.

Fig.8. Anti-inflammatory activity of synthesized compounds (9 a-k)

Fig.1.

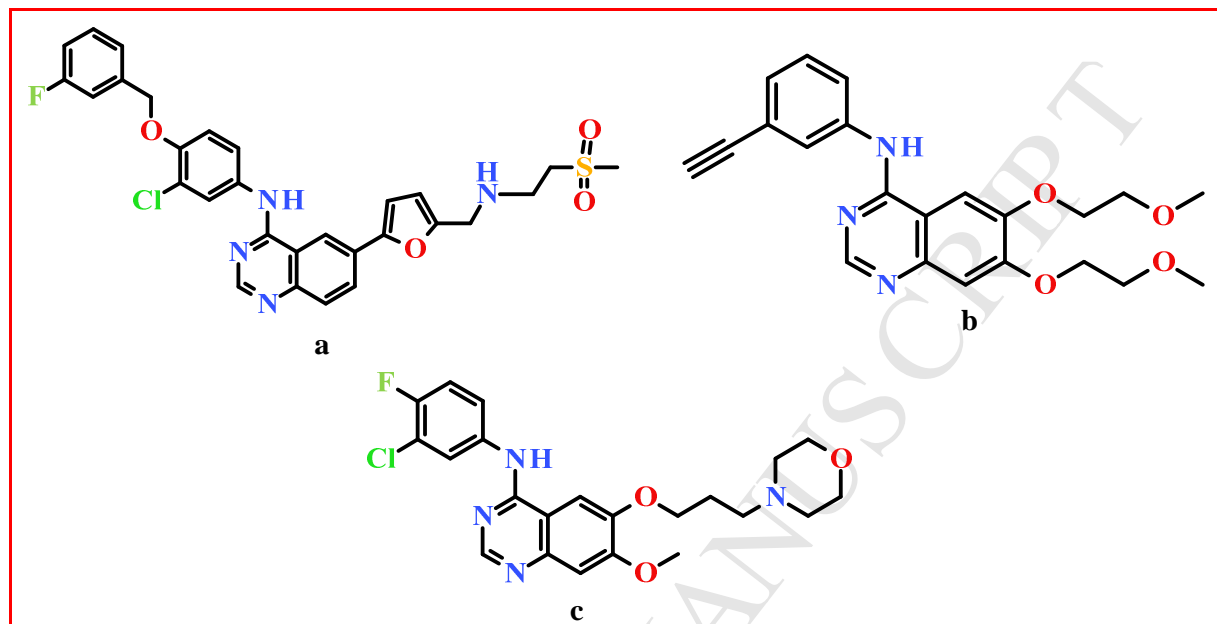


Fig.2.

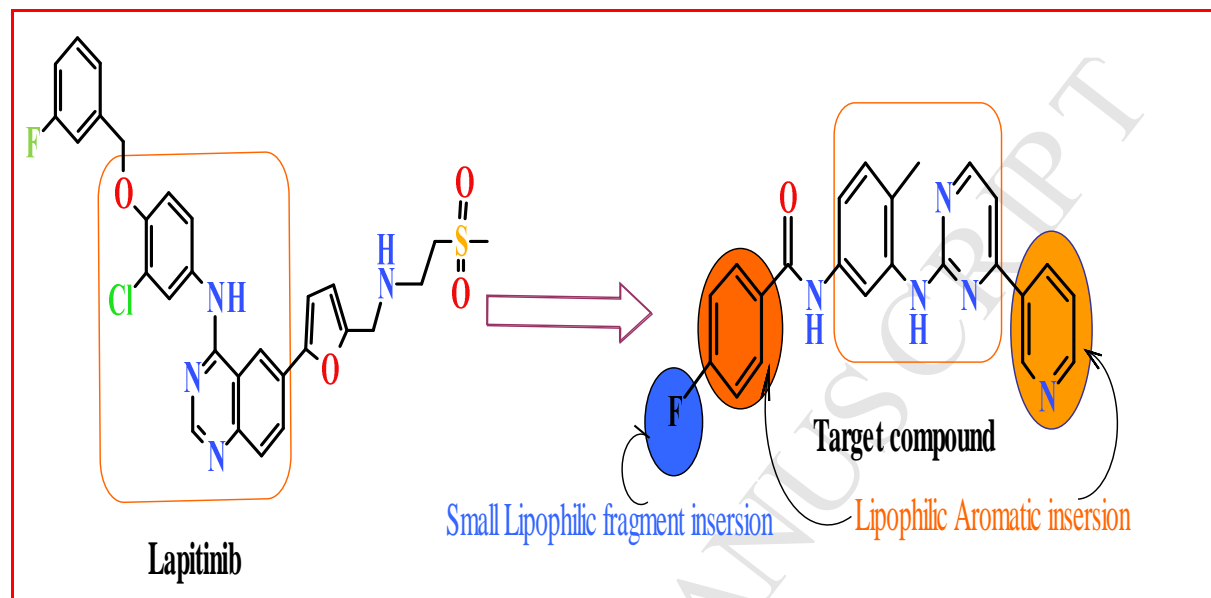


Fig.3.

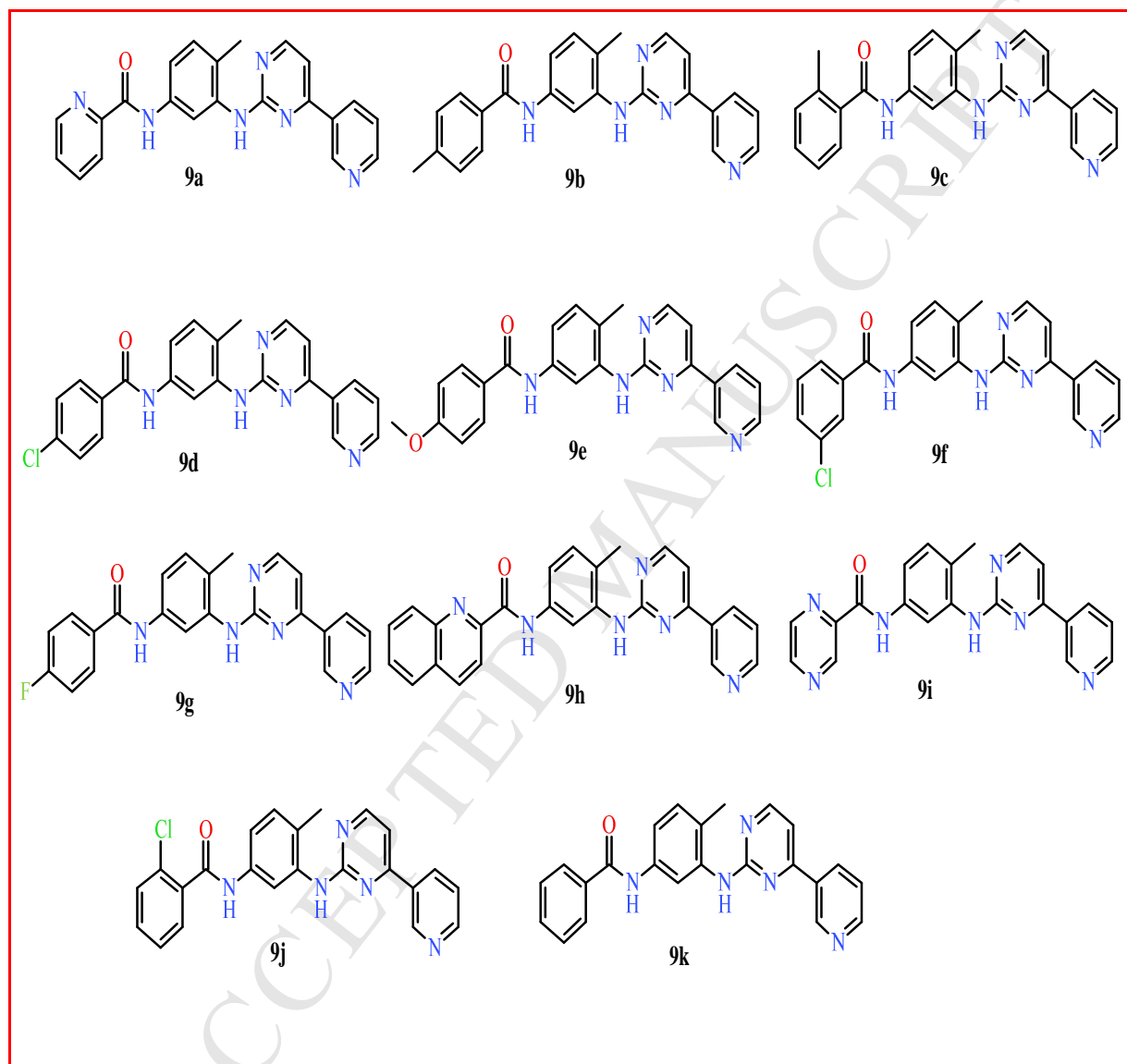


Fig.4.

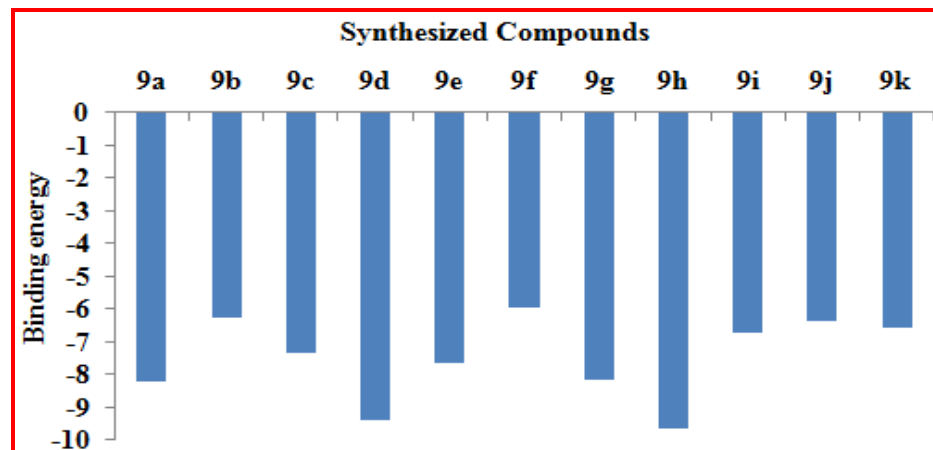


Fig.5.

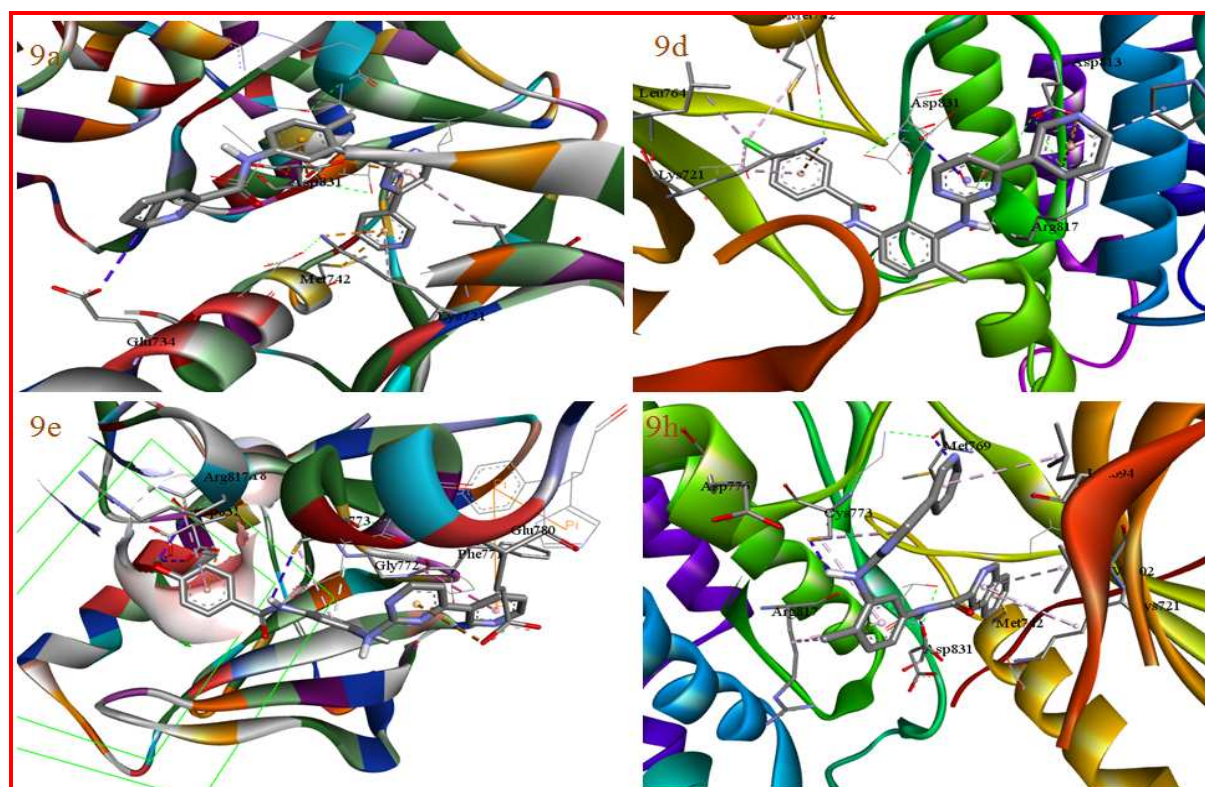


Fig.6.

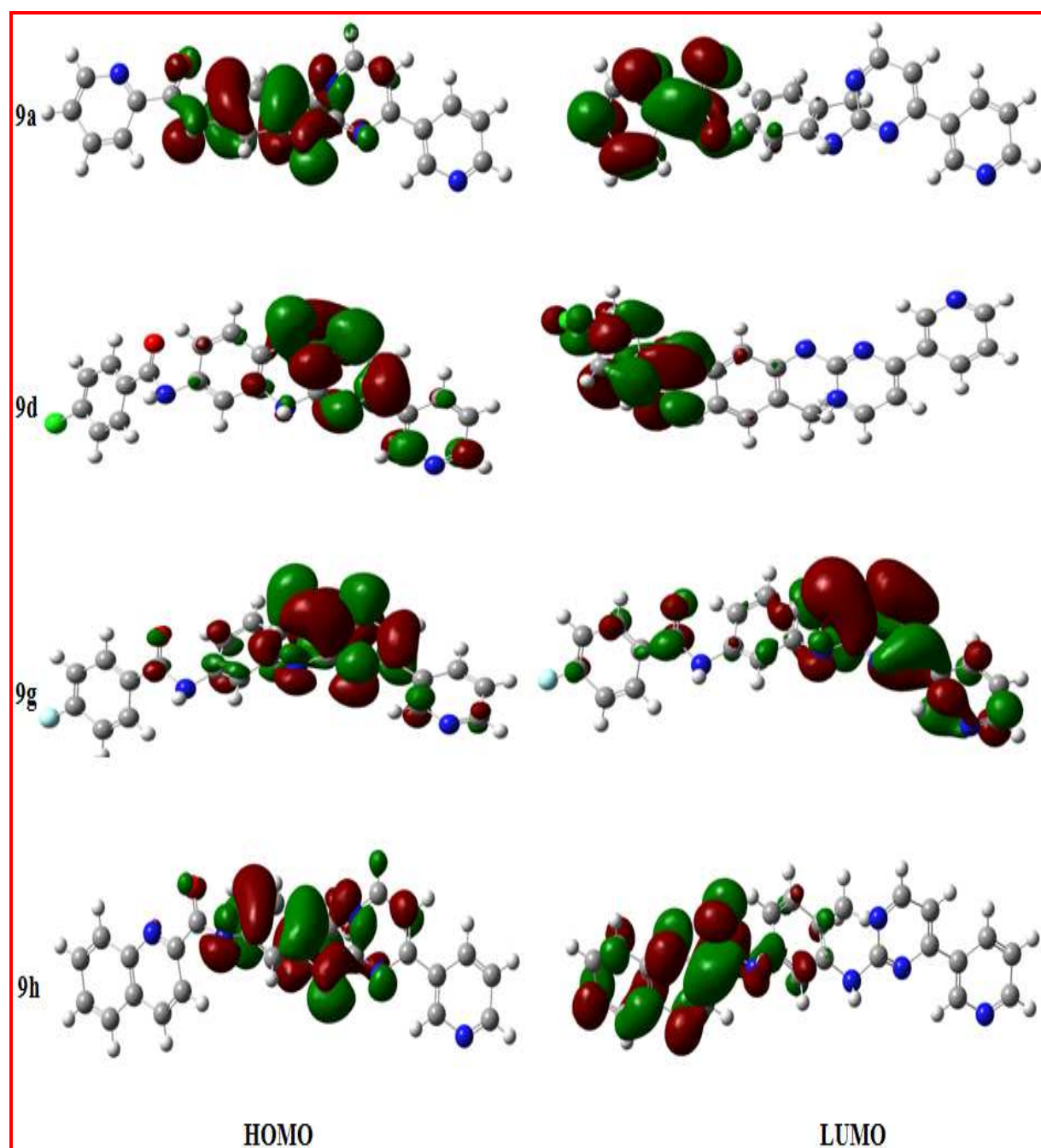


Fig.7.

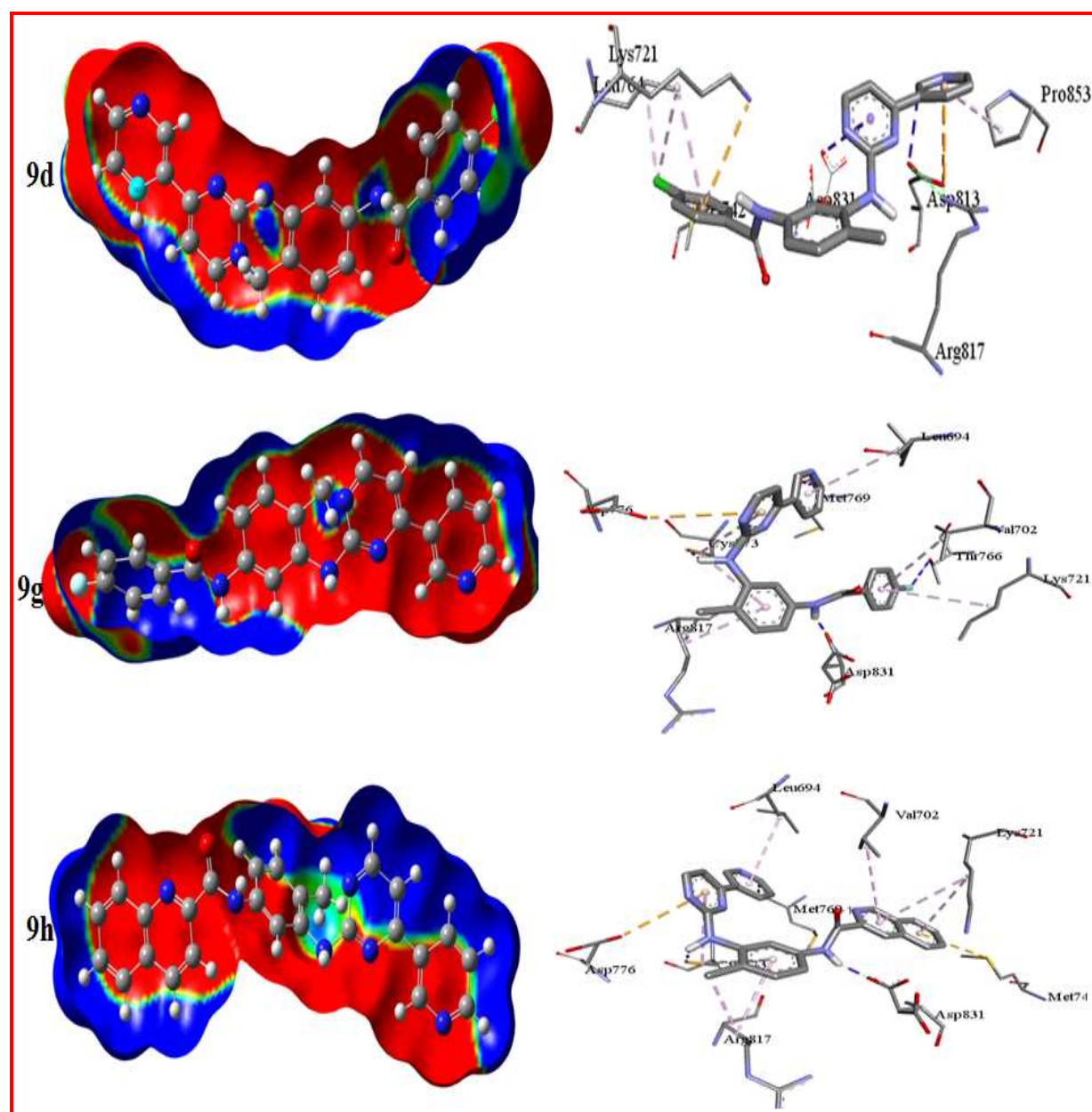
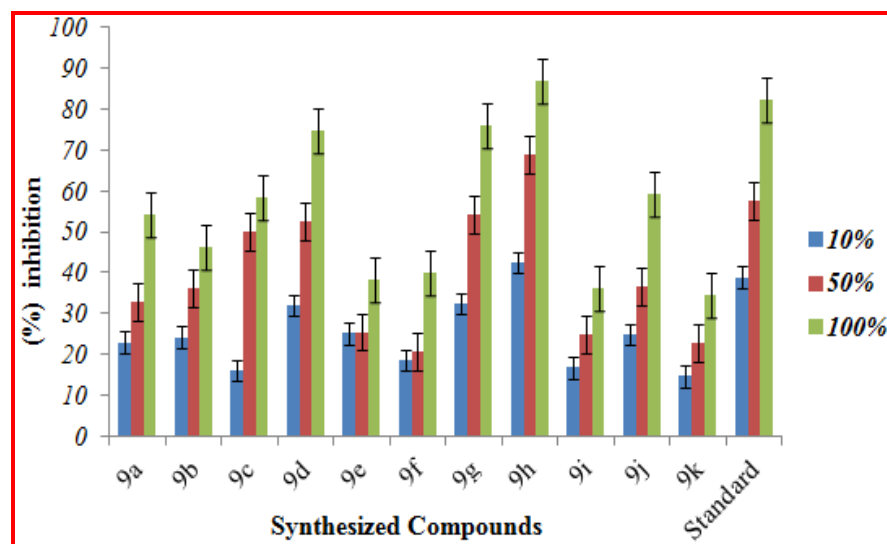
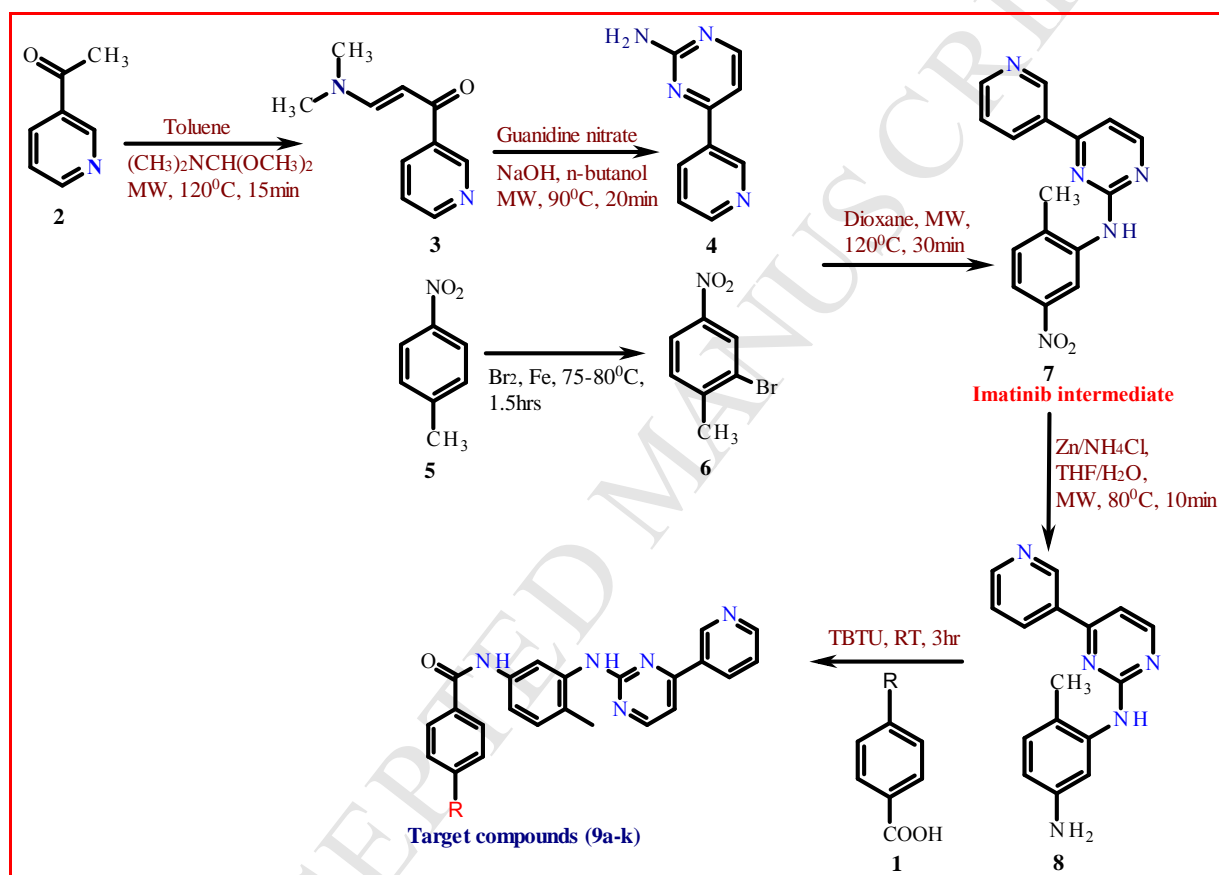


Fig.8.



SCHEME CAPTIONS

Scheme.1. Synthesis of pyrimidine scaffold benzamide derivatives (9 a-k)



Scheme.1.

HIGHLIGHTS

- Synthesized Novel pyrimidine scaffold benzamide derivatives (9a-k)
- *In silico* studies exhibited good binding energy towards the target receptor EGFR (1m17) inhibitor.
- HOMO-LUMO energy gap of the compounds was investigated using the B3LYP/6-31G method.
- Most reactive sites are predicted by using MEPs plot